Physicochemical Characterization of New Sulfate Ionic Liquids

Begoña González,*,† Elena Gómez,‡ Ángeles Domínguez,† Miguel Vilas,§ and Emilia Tojo§

Departamento de Ingeniería Química, Universidad de Vigo, 36310 Vigo, Spain, Laboratory of Separation and Reaction Engineering, Departamento de Engenharia Quimica, Facultade de Engenharia, Universidade do Porto, Rua Dr. Roberto Frias, 4200-465 Porto, Portugal, and Department of Organic Chemistry, University of Vigo, Vigo 36310, Spain

In this work, the ionic liquids 1-ethyl-1-methylpyrrolidinium ethylsulfate [EMpyr][ESO_4], 1-*n*-butyl-1-ethylpyrrolidinium ethylsulfate [BEpyr][ESO_4], 1-*n*-butyl-1-methylpyrrolidium methylsulfate [BMpyr][MSO_4], and triethylmethylammonium methylsulfate [E_3MN][MSO_4] were synthesized, and their experimental densities, speeds of sound, dynamic viscosities, and refractive indices were studied as a function of temperature at atmospheric pressure. Thermal expansion coefficient, molar volume, and molar refraction of these ionic liquids were calculated from the experimental density and refractive index values. A thermal analysis for pyrrolidinium and ammonium-based ionic liquids at temperatures between $T =$ (253.15 and 363.15) K is presented.

Introduction

Information about physical properties of pure liquids and mixtures and their dependence on composition and temperature are important basic data used in chemical engineering designs. Density and viscosity are, among other properties, important physical properties in the design of multiple processes. Ionic liquids (ILs) are room temperature molten salts with unusual properties that include very low vapor pressures. This and other properties make the ILs an important alternative to the organic solvents for different processes,[1,2] and they are being used as separation agents with very promising results, but experimental data of physical properties[3−10] are still scarce. Alkylsulfate-based ILs are some of the most promising ILs to be applied in industrial processes,[11] since most of these ILs can be easily synthesized at a reasonable cost. Furthermore, some of these compounds have an unusually high dielectric constant, a relatively large electrochemical window, are useful as reaction medium.[12] The alkylsulfate-based ILs are widely used in the extraction processes, especially in the petrochemical field; for example, the extraction of sulfur and nitrogen compounds from gasoline and diesel,[13,14] the extraction of aromatic compounds from alkanes,[15−20] or the purification of gasoline octane boosters.[11]

In this paper four new ILs, 1-ethyl-1-methylpyrrolidinium ethylsulfate [EMpyr][ESO_4] (**1**), 1-*n*-butyl-1-ethylpyrrolidinium ethylsulfate [BEpyr][ESO_4] (**2**), 1-*n*-butyl-1-methylpyrrolidium methylsulfate [BMpyr][MSO_4] (**3**), and triethylmethylammonium methylsulfate [E_3MN][MSO_4] (**4**), are synthesized and characterized (Figure 1). As a continuation of our works[21−27] about the ILs physical, thermodynamic, and transport properties, experimental densities, speeds of sound, refractive indices, and dynamic viscosities have been determined at several temperatures for four ILs. These ILs are new, and therefore their physical properties are not available in the literature. From the experimental densities and refractive indices, the thermal expansion coefficients, the molar volumes, and the molar refractions have been calculated at ranging from $T =$ (298.15 to 343.15) K. The obtained results were analyzed to determine the effect of temperature, and the influence of the alkyl chain of cation on these properties. Besides, melting and freezing temperatures of the studied ILs were determined by differential scanning calorimetry.

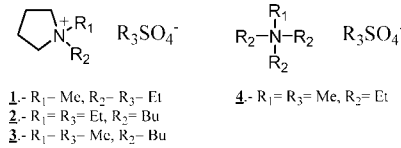

Figure 1. Structure of the ionic liquids synthesized: **1**, [EMpyr][ESO_4]; **2**, [BEpyr][ESO_4]; **3**, [BMpyr][MSO_4]; and **4**, [E_3MN][MSO_4].

Experimental Section

Chemicals. Reagents used for the synthesis of ILs were supplied by Aldrich for 1-butylpyrrolidine ($w > 0.980$), by Fluka for triethylamine ($w > 0.995$), 1-methylpyrrolidine ($w > 0.99$), dimethylsulfate ($w > 0.990$), and diethylsulfate ($w > 0.990$) and by Merck for toluene ($w > 0.999$) and ethyl acetate ($w > 0.995$). These chemicals were of commercial grade and used as such without any purification.

General Procedure for the Synthesis of Alkylpyrrolidinium and Alkylammonium Alkylsulfates. All ILs were prepared according to the following procedure:

Dialkyl sulfate was added dropwise to a solution of equal molar amounts of trialkylamine or alkylpyrrolidine in toluene (15 mL per 0.02 mol of starting amine), and the mixture was cooled in an ice-bath under argon at a rate to maintain the reaction temperature below 313.15 K. The reaction mixture was stirred at room temperature for (1 to 20) h depending on the starting reagents (progress of the reaction was monitored by thin layer chromatography). The upper organic phase of the resulting mixture was decanted, and the lower IL phase was washed with ethyl acetate. After washings, remaining ethyl acetate was removed by heating under reduced pressure. To remove organic solvents and water content to negligible values

* To whom correspondence should be addressed. E-mail: bgp@uvigo.es. Tel.: +34 986 812 422. Fax: +34 986 812 382.
† Departamento de Ingeniería Química, Universidad de Vigo.
‡ Universidade do Porto.
§ Department of Organic Chemistry, University of Vigo.

10.1021/je1006357
Published on Web 12/17/2010

(mass fraction of water determined using a 756 Karl Fisher coulometer) vacuum ($2 \cdot 10^{-1}$ Pa) and moderate temperature (343.15 K) were applied to ILs for several days, always immediately prior to their use. The ILs were kept in bottles under argon gas, in a glovebox.

All ILs were obtained with more than 99% of purity. Their structures were confirmed by ^{1}H NMR and ^{13}C NMR spectroscopy, as well as mass spectrometry. No signals of unreacted starting materials were observed in the NMR spectra. The MS spectra showed peaks due to the association of ions and the presence of ^{34}S and ^{13}C ([M + 1] peak) isotopes.

1-Ethyl-1-methylpyrrolidinium Ethylsulfate [EMpyr][ESO$_4$] (1). Reagents: 1-methylpyrrolidine (2.2 mL, 20.89 mmol) and diethylsulfate (2.7 mL, 20.89 mmol). Reaction time: 3 h. The yield was 90.5% (4.52 g). ^{1}H NMR (400 MHz, $CDCl_3$, ppm, δ): 3.98 [q, 2H, J = 7.1 Hz, OCH_2CH_3], 3.60 [m, 4H, H-2], 3.54 [q, 2H, J = 7.3 Hz, NCH_2CH_3], 3.09 [s, 3H, NCH_3], 2.21 [m, 4H, H-3] 1.36 [t, 3H, J = 7.3 Hz, NCH_2CH_3], 1.20 [t, 3H, J = 7.1 Hz, OCH_2CH_3]. ^{13}C NMR (100.6 MHz, $CDCl_3$, ppm, δ): 63.7, 63.0, 59.3, 47.7, 21.7, 15.3, 9.4. HRMS-ESI m/z (%): 1071 $[(EMpyr)_5(ESO_4)_4]^+$ (**1**), 831 $[(EMpyr)_4(ESO_4)_3]^+$ (**4**), 592 $[(EMpyr)_3(ESO_4)_2]^+$ (**3**), 354 $[(EMpyr)_2(ESO_4) + 1]^+$ (**13**), 353.24685 $[(EMpyr)_2(ESO_4)]^+$ ($C_{16}H_{37}N_2O_4S$ requires 353.24666, 100). Mass fraction of water less than 9×10^{-4}.

1-n-Butyl-1-ethylpyrrolidinium Ethylsulfate [BEpyr][ESO$_4$] (2). Reagents: 1-butylpyrrolidine (2.8 mL, 17.77 mmol) and diethylsulfate (2.3 mL, 17.77 mmol). Reaction time: 20 h. The yield was 92% (4.6 g). ^{1}H NMR (400 MHz, $CDCl_3$, ppm, δ): 4.08 [q, 2H, J = 7.1 Hz, OCH_2CH_3], 3.68 [m, 4H, H-2], 3.48 [q, 2H, J = 7.3 Hz, NCH_2CH_3], 3.30 [m, 2H, NCH_2], 2.26 [m, 4H, H-3], 1.68 [m, 2H, NCH_2CH_2], 1.45 [sextuplet, 2H, J = 7.4 Hz, $N(CH_2)_2CH_2$], 1.38 [t, 3H, J = 7.3 Hz, NCH_2CH_3], 1.28 [t, 3H, J = 7.1 Hz, OCH_2CH_3], 0.99 [t, 3H, J = 7.4 Hz, $N(CH_2)_3CH_3$]. ^{13}C NMR (100.6 MHz, $CDCl_3$, ppm, δ): 62.9, 62.3, 58.9, 54.7, 25.3, 21.9, 19.7, 15.3, 13.6, 9.0. HRMS-ESI m/z (%): 1281 $[(BEpyr)_5(ESO_4)_4]^+$ (**8**), 1000 $[(BEpyr)_4(ESO_4)_3]^+$ (**28**), 719 $[(BEpyr)_3(ESO_4)_2]^+$ (**13**), 438 $[(BEpyr)_2(ESO_4) + 1]^+$ (**21**), 437.34057 $[(BEpyr)_2(ESO_4)]^+$ ($C_{22}H_{49}N_2O_4S$ requires 437.34030, 100). Mass fraction of water less than 7×10^{-4}.

1-n-Butyl-1-methylpyrrolidinium Methylsulfate [BMpyr][MSO$_4$] (3). Reagents: 1-butylpyrrolidine (3.1 mL, 19.73 mmol) and dimethylsulfate (1.9 mL, 19.73 mmol). Reaction time: 4.5 h. The yield was 97.5% (4.87 g). ^{1}H NMR (400 MHz, $CDCl_3$, ppm, δ): 3.65 [s, 3H, OCH_3], 3.62 [m, 4H, H-2], 3.43 [m, 2H, NCH_2], 3.12 [s, 3H, NCH_3], 2.23 [m, 4H, H-3], 1.72 [m, 2H, NCH_2CH_2], 1.39 [sextuplet, 2H, J = 7.4 Hz, $N(CH_2)_2CH_2$], 0.95 [t, 3H, J = 7.4 Hz, $N(CH_2)_3CH_3$]. ^{13}C NMR (100.6 MHz, $CDCl_3$, ppm, δ): 64.2, 63.9, 54.2, 48.2, 25.8, 21.6, 19.6, 13.6. HRMS-ESI m/z (%): 1408 $[(BMpyr)_6(MSO_4)_5]^+$ (**3**), 1155 $[(BMpyr)_5(MSO_4)_4]^+$ (**15**), $[(BMpyr)_5(MSO_4)_4]^+$ (**15**), 902 $[(BMpyr)_4(MSO_4)_3]^+$ (**36**), 648 $[(BMpyr)_3(MSO_4)_2]^+$ (**6**), 397 $[(BMpyr)_2(MSO_4) + 2]^+$ (**3**), 396 $[(BMpyr)_2(MSO_4) + 1]^+$ (**2**), 395.29380 $[(BMpyr)_2(MSO_4)]^+$ ($C_{19}H_{43}N_2O_4S$ requires 395.29344, 100). Mass fraction of water less than 6×10^{-4}.

Triethylmethylammonium Methylsulfate [E$_3$MN][MSO$_4$] (4). Reagents: triethylamine (3.1 mL, 21.9 mmol) and dimethylsulfate (2.1 mL, 21.9 mmol). Reaction time: 1 h. The yield was 98% (4.9 g). ^{1}H NMR (400 MHz, $CDCl_3$, ppm, δ): 3.61 [s, 3H, OCH_3], 3.38 [q, 6H, J = 7.3 Hz, NCH_2CH_3], 3.02 [s, 3H, NCH_3], 1.31 [t, 9H, J = 7.3 Hz, NCH_2CH_3]. ^{13}C NMR (100.6 MHz, $CDCl_3$, ppm, δ): 55.5 [t, J(C,N)= 2.6 Hz], 53.9, 46.4 [t, J(C,N)= 4.0 Hz], 7.6. HRMS-ESI m/z (%): 1252 $[(E_3MN)_6(MSO_4)_5]^+$ (**4**), 1025 $[(E_3MN)_5(MSO_4)_4]^+$ (**6**), 797 $[(E_3MN)_4(MSO_4)_3]^+$ (**19**), 570 $[(E_3MN)_3(MSO_4)_2]^+$ (**8**), 345 $[(E_3MN)_2(MSO_4) + 2]^+$ (**1**), 344 $[(E_3MN)_2(MSO_4) + 1]^+$ (**13**), 343.26250 $[(E_3MN)_2(MSO_4)]^+$ ($C_{15}H_{39}N_2O_4S$ requires 343.26212, 100). Mass fraction of water less than 7×10^{-4}.

NMR spectra were measured on a Bruker ARX 400 and Electrospray MS were recorded on a Bruker FTMS APEX/Qe mass spectrometer. Figure 1 shows the structure of the ILs synthetized.

Apparatus and Procedure. DSC. Measurement of phase transition temperatures were performed using a Mettler-Toledo differential scanning calorimeter (DSC), model DSC822^e, and the data were evaluated using the Mettler-Toledo STAR^e software version 8.01. The instrument was calibrated for temperature and heat flow with zinc and indium reference samples provided by Mettler-Toledo. The presence of volatiles affects the glass transition and melting temperatures,[28,29] therefore a known mass of sample ((4 to 8) mg) was placed in an aluminum pan, and it was dried in situ on the DSC by holding the sample at T = 383.15 K for 30 min. This process was repeated until the weight of the sample remained constant. Aluminum pans of 40 μL with a pinhole at the top hermetically sealed were used. The sample pan and blank (an empty pan) were placed on separated raised platforms within the furnace and they were exposed to a flowing N_2 atmosphere. Measurements for melting and freezing temperatures were determined by cooling the samples from (383.15 to 253.15) K, at a rate of 2 K/min, followed by heating from (253.15 to 363.15) K at a rate of 10 K/min.

For the determination of the uncertainty in the temperature measurements, three consecutive scans of the same sample, and three scans removing and replacing the pan, were carried out; the variability in the measured temperatures was ($\pm$0.2 and $\pm$0.3) K, respectively. Taking into account that small impurities in ILs can affect their thermal properties, and that the scan rate has influence on the results, the overall uncertainty for the temperature measurement was estimated to be $\pm$1 K.

Densities and Speeds of Sound. Densities and speeds of sound of the ILs were measured using an Anton Paar DSA-5000 digital vibrating-tube densimeter. The DSA-5000 automatically corrects the influence of viscosity on the measured density. The repeatability and uncertainty in experimental measurements have been found to be lower than ($\pm 2 \cdot 10^{-6}$ and $\pm 3 \cdot 10^{-5}$) g·cm^{-3} for the density and ($\pm$0.01 and $\pm$0.3) m·s^{-1} for the speed of sound, respectively. The apparatus was calibrated by measuring the density of Millipore quality water and ambient air according to the manual instructions. The calibration was checked with known density and speed of sound of pure liquids.

Refractive Indices. To measure refractive indices, an automatic refractometer Abbemat-HP Dr. Kernchen with a resolution of $\pm 10^{-6}$ and an uncertainty in the experimental measurements of $\pm 4 \cdot 10^{-5}$ was used. The apparatus was calibrated by measuring the refractive index of Millipore quality water and tetrachloroethylene (provided by the supplier) before each series of measurements, according to manual instructions. The calibration was checked with known refractive index of pure liquids.

Dynamic Viscosities. Kinematic viscosities were determined using an automatic viscosimeter Lauda PVS1 with three Ubbelhode capillary microviscosimeters of ($0.53 \cdot 10^{-3}$, $0.70 \cdot 10^{-3}$, and $1.26 \cdot 10^{-3}$) m diameter (the uncertainty in experimental measurement was ($\pm$0.01, $\pm$ 0.03, and $\pm$0.2) mPa·s, respectively). Gravity fall is the principle of measurement on which this viscosimeter is based. The capillary was maintained in a D20KP LAUDA thermostat with an uncertainty of 0.01 K. The capillaries were calibrated and credited by the

Table 1. Melting (T_m) and Freezing (T_f) Temperatures for the Pure ILs

IL	T_m / K	T_f / K
BuEtPyr $EtSO_4$	311	292
EtMePyr $EtSO_4$	298	283
BuMePyr $MeSO_4$		
Et_3MeN $MeSO_4$	298	293

company. The equipment has a control unit PVS1 (Processor Viscosity System) that is a PC-controlled instrument for the precise measurement of the fall time, using standardized glass capillaries, with an uncertainty of 0.01 s. In order to verify the calibration, viscosity of pure liquids were compared with literature data.

Results and Discussion

DSC. The results from the thermal analysis are presented in Table 1. In this table, the melting temperatures (T_m) and freezing temperatures (T_f) were determined as the onset temperature of an endothermic curve on heating, and the onset temperature of an exothermic curve on cooling, respectively. [BEpyr][ESO_4], [E_3MN][MSO_4], and [EMpyr][ESO_4] present freezing and melting transitions, while [BMpyr][MSO_4] does not exhibit phase transitions in the studied temperature range. As an example, the DSC scan for [E_3MN][MSO_4] is presented in Figure 2. Figure 2a shows freezing point on cooling whereas 2b shows melting point on heating, for this IL. Among these ILs, the influence of the length of alkyl chain can also be studied by comparing the behavior of the thermal properties of [BEpyr][ESO_4], and [EMpyr][ESO_4]. It is observed that increase in length of alkyl chain causes an increase in melting and freezing temperatures.

Density, Speed of Sound, Refractive Index, and Dynamic Viscosity. Densities, speeds of sound, dynamic viscosities and refractive indices of [EMpyr][ESO_4], [BEpyr][ESO_4], [BMpyr]-[MSO_4], and [E_3MN][MSO_4] ionic liquids were experimentally

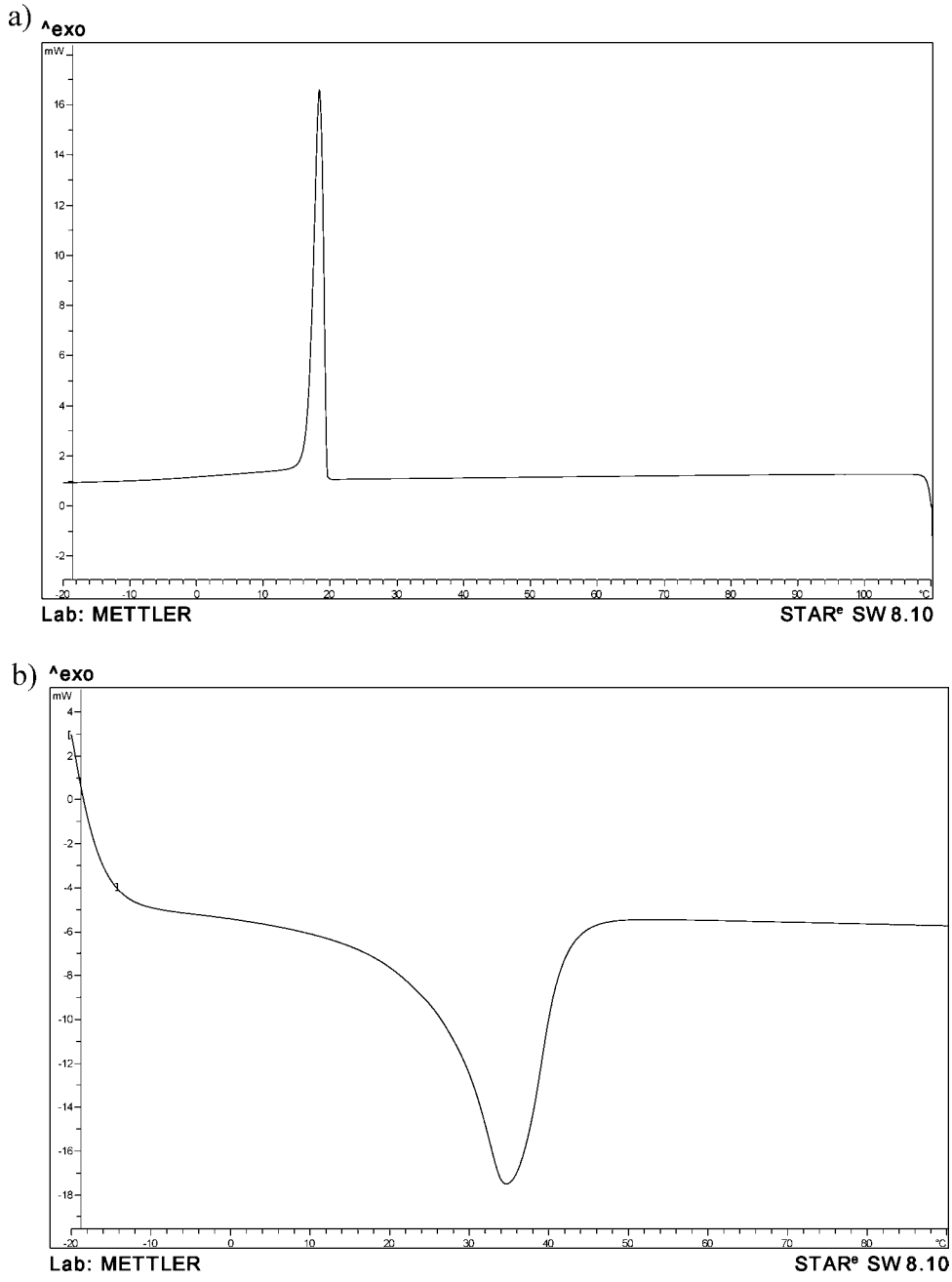

Figure 2. DSC scan for [E_3MN][MSO_4] (a) cooling and (b) heating.

measured from their melting temperature (in their liquid range), given in Table 1, and atmospheric pressure. The obtained values are summarized in Table 2.

The following equations were used to fit the density, ρ (eq 2), the refractive index, n_D (eq 1), and the speed of sound, u (eq 1), with temperature:

$$z = a + \mathrm{bT} \tag{1}$$

$$z = a + bT + cT^2 \tag{2}$$

where z is ρ, n_D or u, T is the absolute temperature, and a, b, and c are adjustable parameters. The characteristic parameters a, b, and c are given in Table 3 together with the standard relative deviations, srd

$$\mathrm{srd} = \left\{ \sum_{\mathrm{i}}^{\mathrm{n_{dat}}} \left(\frac{(\mathrm{z} - \mathrm{z_{cal}})}{\mathrm{z}} \right)^2 / n_{\mathrm{dat}} \right\}^{1/2} \tag{3}$$

where z and z_{cal} are the values of the experimental and calculated property, and n_{dat} is the number of experimental points.

The viscosity values, η, were fitted using Arrehenius-like law and Vogel−Fulcher−Tamman (VFT) equations. The most commonly used equation to correlate the variation of viscosity with temperature is the Arrhenius-like law

$$\eta = \eta_\infty \exp\left(\frac{-E_a}{RT}\right) \tag{4}$$

In this equation the viscosity at infinite temperature, η_∞, and the activation energy, E_a, are characteristic parameters generally adjusted from experimental data. According to Seddon et al.,[30] the Arrhenius law can generally be applied when the cation presents only a limited symmetry. If this is not the case, and especially in the presence of symmetrical cations, Vogel−Fulcher−Tamman (VFT) equation is recommended[31,32]

$$\eta = AT^{0.5} \exp\left(\frac{k}{(T - T_0)}\right) \tag{5}$$

where A, k, and T_0 are adjustable parameters. Table 4 lists the parameters for these equations together with the standard relative deviations (srd, eq 3). It is evident from Table 4 that VFT gives the best fit for viscosity data. However, for [BEpyr][ESO_4] IL, Arrenhius equation also gives good results.

Figures 3 to 6 show the variation of density, speed of sound, refractive index, and dynamic viscosity with the temperature for all the four ILs: [EMpyr][ESO_4], [BEpyr][ESO_4], [BMpyr][MSO_4], and [E_3MN][MSO_4]. It is observed from these figures that the studied physical properties decrease with the increase in temperature.

Table 2. Density, ρ, Refractive Index, n_D, Speed of Sound, u, and Dynamic Viscosity, η, of [EMpyr][ESO_4], [BEpyr][ESO_4], [BMpyr][MSO_4], and [E_3MN][MSO_4] at Several Temperatures

T/K	ρ/g·cm^{-3}	$10^3\,\eta$/Pa·s	n_D	u/m·s^{-1}	T/K	ρ/g·cm^{-3}	$10^3\,\eta$/Pa·s	n_D	u/m·s^{-1}
	[EMpyr][ESO_4]					[BEpyr][ESO_4]			
308.15	1.18967	172.0	1.47021	1750.2					
313.15	1.18653	134.9	1.46891	1737.5					
318.15	1.18341	107.5	1.46760	1725.2					
323.15	1.18030	86.8	1.46632	1713.0					
328.15	1.17722	71.2	1.46506	1701.0	328.15	1.11872	105.5	1.46710	1602.0
333.15	1.17415	59.1	1.46378	1689.2	333.15	1.11598	82.9	1.46581	1589.6
338.15	1.17111	49.5	1.46246	1677.3	338.15	1.11302	66.8	1.46454	1577.2
343.15	1.16807	42.0	1.46116	1665.7	343.15	1.11008	55.8	1.46315	1564.9
	[BMpyr][MSO_4]					[E_3MN][MSO_4]			
298.15	1.16669	467.5	1.47308	1741.6					
303.15	1.16358	334.9	1.47184	1727.3					
308.15	1.16046	245.6	1.47054	1713.6	308.15	1.16644	218.5	1.46191	1853.5
313.15	1.15740	184.1	1.46924	1700.3	313.15	1.16340	165.6	1.46065	1839.7
318.15	1.15440	139.2	1.46792	1687.4	318.15	1.16036	127.7	1.45939	1826.3
323.15	1.15142	107.8	1.46661	1674.7	323.15	1.15734	100.3	1.45812	1813.1
328.15	1.14842	86.1	1.46536	1662.2	328.15	1.15432	79.7	1.45687	1800.0
333.15	1.14542	69.2	1.46406	1649.8	333.15	1.15133	64.0	1.45561	1787.1
338.15	1.14244	56.4	1.46274	1637.6	338.15	1.14834	53.42	1.45402	1774.2
343.15	1.13947	46.6	1.46143	1625.5	343.15	1.14536	44.92	1.45283	1761.5

Table 3. Fitting Parameters of eq 2 together with the Standard Relative Deviations of the Fit (srd) for the Density, Refractive Index, and Speed of Sound of [EMpyr][ESO_4], [BEpyr][ESO_4], [BMpyr][MSO_4], and [E_3MN][MSO_4]

		a	b/K	c/K^2	srd
[EMpyr][ESO_4]	ρ/g·cm^{-3}	1.419	$-8.59\cdot10^{-4}$	$3.72\cdot10^{-7}$	$1.39\cdot10^{-5}$
	n_D	1.549	$-2.58\cdot10^{-4}$		$9.26\cdot10^{-6}$
	u/m·s^{-1}	$2.491\cdot10^3$	−2.409		$1.50\cdot10^{-4}$
[BEpyr][ESO_4]	ρ/g·cm^{-3}	1.082	$7.72\cdot10^{-4}$	$-2.01\cdot10^{-6}$	$5.74\cdot10^{-5}$
	n_D	1.553	$-2.62\cdot10^{-4}$		$7.22\cdot10^{-5}$
	u/m·s^{-1}	$2.413\cdot10^3$	−2.474		$1.03\cdot10^{-4}$
[BMpyr][MSO_4]	ρ/g·cm^{-3}	1.383	$-8.33\cdot10^{-4}$	$3.57\cdot10^{-7}$	$2.90\cdot10^{-5}$
	n_D	1.550	$-2.59\cdot10^{-4}$		$3.74\cdot10^{-5}$
	u/m·s^{-1}	$2.505\cdot10^3$	−2.569		$5.54\cdot10^{-4}$
[E_3MN][MSO_4]	ρ/g·cm^{-3}	1.377	$-7.55\cdot10^{-4}$	$2.35\cdot10^{-7}$	$9.79\cdot10^{-5}$
	n_D	1.542	$-2.60\cdot10^{-4}$		$6.78\cdot10^{-5}$
	u/m·s^{-1}	$2.661\cdot10^3$	−2.624		$1.68\cdot10^{-4}$

Table 4. Adjustable Parameters of the VFT Equation (A, k, and T_0), and Arrhenius Equation (η_∞, E_a), together with the Standard Relative Deviations of the Fit (srd) for the Viscosity of [EMpyr][ESO_4], [BEpyr][ESO_4], [BMpyr][MSO_4], and [EEEMN][MSO_4]

	VFT equation				Arrhenius equation		
	A	k	T_0		η_∞	$-E_a$	
	mPa·s·$K^{-0.5}$	K	K	srd	mPa·s	J·mol^{-1}	srd
[EMpyr][ESO_4]	0.0084	946.03	174.23	0.002	$3.18 \cdot 10^{-5}$	39860	0.053
[BEpyr][ESO_4]	0.0045	1052.72	180.90	0.005	$4.61 \cdot 10^{-5}$	39900	0.008
[BMpyr][MSO_4]	0.0054	987.82	182.20	0.005	$1.09 \cdot 10^{-5}$	43362	0.037
[EEEMN][MSO_4]	0.0066	946.70	182.72	0.005	$3.66 \cdot 10^{-5}$	39860	0.022

Furthermore, Figure 3 shows that density increase in the order: [BEpyr][ESO_4] < [BMpyr][MSO_4] < [E_3MN][MSO_4] < [EMpyr][ESO_4]. Thus, an increase in the length of alkyl chain of the cation ([BEpyr][ESO_4], [EMpyr][ESO_4]) causes decrease in density. This behavior is in agreement with that of other ILs found in literature.[21,27,33]

The variation of speed of sound with the temperature can be observed in Figure 4. As density, this property decreases with the increase of the alkyl chain length of the cation ([BEpyr][ESO_4], [EMpyr][ESO_4]).

The refractive indices of the ILs studied in this work versus temperature are plotted in Figure 5. As it can be observed over the studied temperature range, the refractive index decreases linearly with temperature. The comparison of refractive index results for [BEpyr][ESO_4] and [EMpyr][ESO_4] in Figure 4 suggests that refractive index increases with increase of alkyl chain length of cation.

Figure 6 depicts the viscosity against the temperature together with the fitting using VFT equation (eq 5), which gives lower deviations. It is evident from Figure that the correlated values are in good agreement with the experimental data. Similar to refractive index, viscosity also increases with increase of alkyl chain length of cation.

Thermodynamic Properties. The change of the molar volume with temperature can be expressed through the coefficient of thermal expansion, α, sometimes called the coefficient of cubical expansion. From the experimental data of densities, ρ, at the temperature range studied, α can be calculated using the following equation:

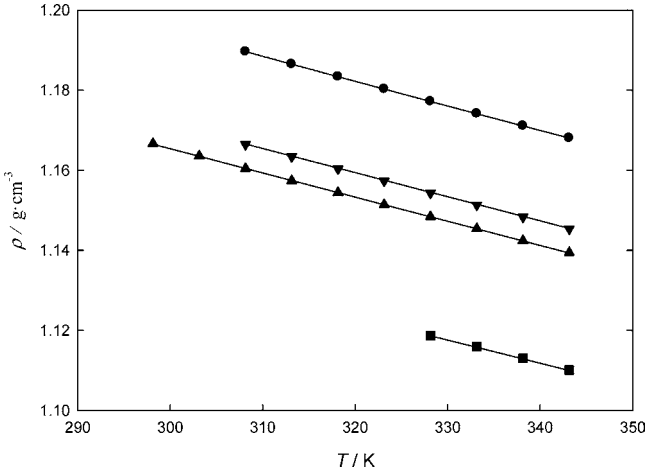

Figure 3. Density, ρ, and fitted curves (−) as a function of temperature. Experimental points: ●, [EMpyr][ESO_4]; ■, [BEpyr][ESO_4]; ▲, [BMpyr]-[MSO_4]; and ▼, [E_3MN][MSO_4].

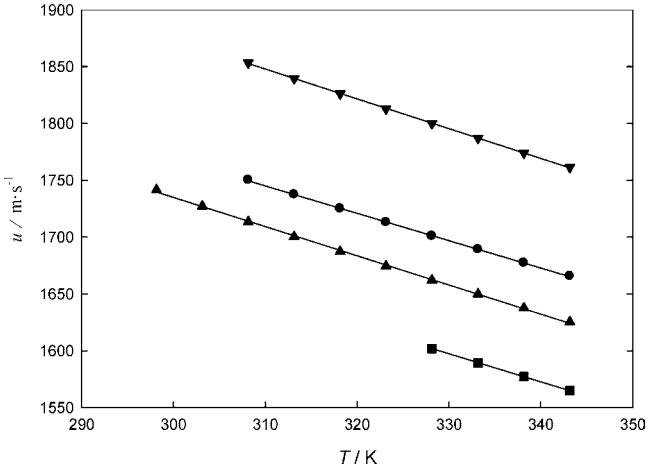

Figure 4. Speed of sound, u, and fitted curves (−) as a function of temperature. Experimental points: ●, [EMpyr][ESO_4]; ■, [BEpyr][ESO_4]; ▲, [BMpyr][MSO_4]; and ▼, [E_3MN][MSO_4].

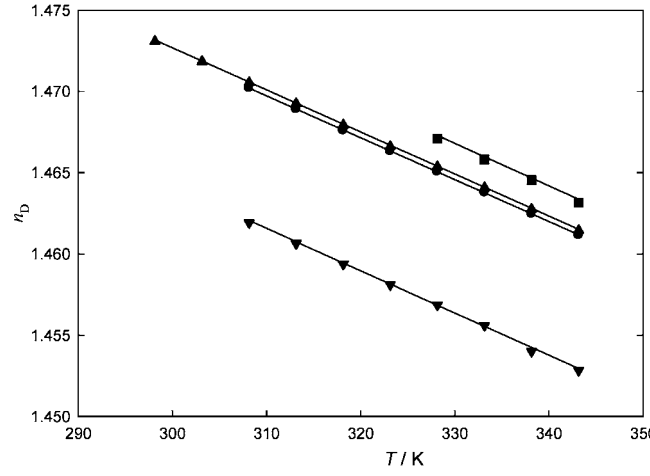

Figure 5. Refractive index, n_D, and fitted curves (−) as a function of temperature. Experimental points: ●, [EMpyr][ESO_4]; ■, [BEpyr][ESO_4]; ▲, [BMpyr][MSO_4]; and ▼, [E_3MN][MSO_4].

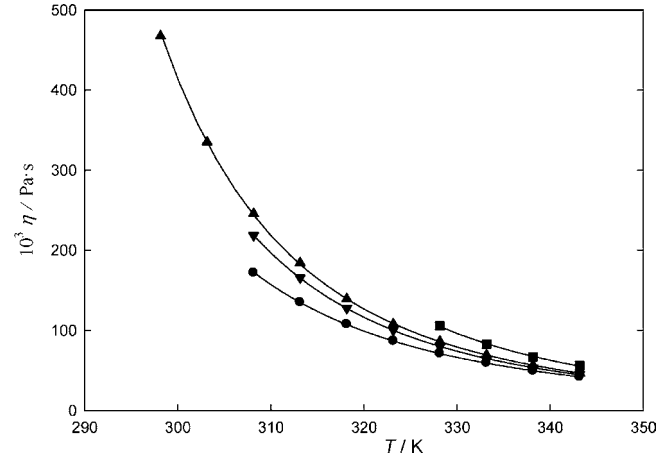

Figure 6. Dynamic viscosity, η, and fitted curves with VFT equation (−) as a function of temperature. Experimental points: ●, [EMpyr][ESO_4]; ■, [BEpyr][ESO_4]; ▲, [BMpyr][MSO_4]; and ▼, [E_3MN][MSO_4].

$$\alpha = -\frac{1}{\rho}\left(\frac{\partial \rho}{\partial T}\right)_P = \left(-\frac{\partial \ln \rho}{\partial T}\right) \quad (6)$$

The α value is obtained from the slope of the representation of *ln ρ* against temperature. It is observed that α value is constant with the temperature, being $\alpha = 5.23\ K^{-1}$ for [EMpyr][ESO_4], $\alpha = 5.18\ K^{-1}$ for [BEpyr][ESO_4], $\alpha = 5.24\ K^{-1}$ for [BMpyr]-[MSO_4], and $\alpha = 5.21\ K^{-1}$ for [E_3MN][MSO_4].

From the experimental densities and refractive indices, the molar refractions of ILs, R_m, were calculated at several temperatures using the Lorenz−Lorentz equation

$$R_m = \left(\frac{{n_D}^2 - 1}{{n_D}^2 + 2}\right)V_m \quad (7)$$

where V_m is the molar volume. Table 5 summarizes the molar refractions, R_m, and molar volumes, V_m, at several temperatures for the pure ILs. From the values presented in this table, it can be concluded that an increase in the temperature means a slight increase of the molar volumes, while the molar refractions are practically constant with the studied temperatures. Further, it is possible to observe, in this Table 5, that an increase in the length of alkyl chain of the cation ([BEpyr][ESO_4], [EMpyr][ESO_4]) causes increase in molar volume. The behavior of the molar volume is in agreement with that of other ILs found in literature.[27,33] Figure 7 shows that an increase in the alkyl chain length ([BEpyr][ESO_4], [EMpyr][ESO_4]) means a slight increase in the values of the molar refractions.

Conclusions

Four new ILs, 1-ethyl-1-methylpyrrolidinium ethylsulfate [EMpyr][ESO_4], 1-*n*-butyl-1-ethylpyrrolidinium ethylsulfate [BEpyr][ESO_4], 1-*n*-butyl-1-methylpyrrolidium methylsulfate [BMpyr][MSO_4], and triethylmethylammonium methylsulfate [E_3MN][MSO_4], were synthesized and presented together with their density, speed of sound, dynamic viscosity and refractive index from $T = (298.15$ to $343.15)$ K at atmospheric pressure. From the experimental densities and refractive indices, the coefficients of thermal expansion, the molar volumes, and the molar refractions have been calculated at several temperatures. The obtained data were analyzed to evaluate the effect of temperature and the influence of the alkyl chain of cation on such properties.

A linear dependence of refractive index and speed of sound and a quasi-linear dependence of density have been found in the range of the measurements for the ILs under study. It can be concluded that all studied properties decreases as the temperature increases. The viscosity values were fitted using Arrehenius-like law and Vogel−Fulcher−Tamman (VFT) equations. Better results were obtained using the VFT equation. As usual, dynamic viscosity decrease as temperature increases.

An increase of the cation alkyl chain length ([BEpyr][ESO_4], [EMpyr][ESO_4]) means a decrease in density and an increase in refractive index and dynamic viscosity. This behavior is in agreement with that of other ILs found in literature.

The melting and freezing temperatures were determined for the ILs presented in this work. From the thermal analysis can be deduced that an increase of the cation alkyl chain length means an increase in the melting and freezing temperatures.

Table 5. Values of Calculated Molar Volumes, V_m, and Molar Refractions, R_m, of [EMpyr][ESO_4], [BEpyr][ESO_4], [BMpyr][MSO_4], and [E_3MN][MSO_4] at Several Temperatures

T	V_m	R_m	V_m	R_m
K	$cm^3 \cdot mol^{-1}$	$cm^3 \cdot mol^{-1}$	$cm^3 \cdot mol^{-1}$	$cm^3 \cdot mol^{-1}$
	[EMpyr][ESO_4]		[BEpyr][ESO_4]	
308.15	296.93	82.88		
313.15	297.71	82.90		
318.15	298.50	82.92		
323.15	299.29	82.94		
328.15	300.07	82.96	390.93	108.49
333.15	300.85	82.98	391.89	108.50
338.15	301.63	83.00	392.93	108.53
343.15	302.42	83.01	393.97	108.54
	[BMpyr][MSO_4]		[E_3MN][MSO_4]	
298.15	338.82	95.06		
303.15	339.72	95.10		
308.15	340.63	95.13	294.28	80.89
313.15	341.54	95.16	295.05	80.91
318.15	342.42	95.17	295.82	80.93
323.15	343.31	95.19	296.60	80.95
328.15	344.21	95.22	297.37	80.97
333.15	345.11	95.24	298.14	80.99
338.15	346.01	95.25	298.92	80.95
343.15	346.91	95.27	299.70	80.98

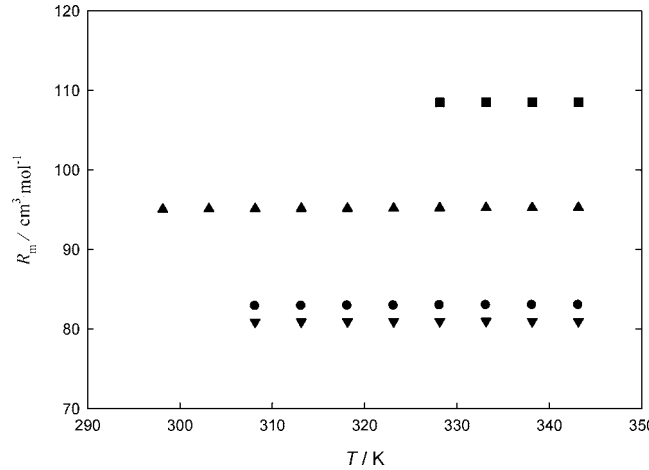

Figure 7. Refractive molar, R_m, as a function of temperature. Experimental points: ●, [EMpyr][ESO_4]; ■, [BEpyr][ESO_4]; ▲, [BMpyr][MSO_4]; and ▼, [E_3MN][MSO_4].

Literature Cited

(1) Zaitsau, D. H.; Kabo, G. J.; Strecha, A. A.; Paulechka, Y. U.; Tschersich, A.; Verevkin, S. P.; Heintz, A. Experimental vapour pressures of 1-alkyl-3-methylimidazoliym bis(trifluoromethylsulfonyl)imides and a correlation scheme for estimation of vaporization enthalpies of ionic liquids. *J. Phys. Chem. A* **2006**, *110*, 7303–7306.

(2) Rebelo, L. P. N.; Lopes, J. N. C.; Esperança, J. M. S. S.; Filipe, E. On the critical temperature, normal boiling point, and vapour pressure of ionic liquids. *J. Phys. Chem. B* **2005**, *109*, 6040–6043.

(3) Wu, T.-Y.; Su, S.-G.; Gung, S.-T.; Lin, M.-W.; Lin, Y.-C.; Lai, C.-A.; Sun, I.-W. Ionic liquids containing an alkyl sulfate group as potential electrolytes. *Electrochim. Acta* **2010**, *55*, 4475–4482.

(4) Ziyada, A. K.; Wilfred, C. D.; Bustam, M. A.; Man, Z.; Murugesan, T. Thermophysical properties of 1-propyronitrile-3-alkylimidazolium bromide Ionic Liquids at temperatures from (293.15 to 353.15) K *J. Chem. Eng. Data* **2010**, DOI: 10.1021/je901050v.

(5) Papaiconomou, N.; Estager, J.; Bauduin, P.; Bas, C.; Roche, S.; Viboud, S.; Draye, M. Synthesis, physicochemical properties, and toxicity data of new hydrophobic ionic liquids containing dimethylpyridinium and trimethylpyridinium cations. *J. Chem. Eng. Data* **2010**, *55*, 1971–1979.

(6) Tsunashima, K.; Niwa, E.; Kodama, S.; Sugiya, M.; Ono, Y. Thermal and transport properties of ionic liquids based on benzyl-substituted phosphonium cations. *J. Phys. Chem. B* **2009**, *113*, 15870–15874.

(7) Blesic, M.; Swadzba-Kwasny, M.; Belhocine, T.; Gunaratne, H. Q. N.; Lopes, J. N. C.; Gomes, M. F. C.; Padua, A. A. H.; Seddon, K. R.; Rebelo, L. P. N. 1-Alkyl-3-methylimidazolium alkanesulfonate ionic liquids, [CnH2n+1mim][CkH2k+1SO3]: synthesis and physicochemical properties. *Phys. Chem. Chem. Phys.* **2009**, *11*, 8939–8948.

(8) Galan Sanchez, L.; Ribe Espel, J.; Onink, F.; Meindersma, G. W.; de Haan, A. B. Density, viscosity, and surface tension of synthesis grade

imidazolium, pyridinium, and pyrrolidinium based room temperature ionic liquids. *J. Chem. Eng. Data* **2009**, *54*, 2803–2812.
(9) Zang, S. L.; Fang, D. W.; Li, J. X.; Zhang, Y. Y.; Yue, S. The estimation of physico-chemical properties of ionic liquid N-propylpyridine rhenate. *Fluid Phase Equilib.* **2009**, *283*, 93–96.
(10) Anouti, M.; Caillon-Caravanier, M.; Le Floch, C.; Lemordant, D. Alkylammonium-based protic ionic liquids. II. Ionic transport and heat-transfer properties: fragility and ionicity rule. *J. Phys. Chem. B* **2008**, *112*, 9412–9416.
(11) Arce, A.; Rodriguez, H.; Soto, A. Use of a Green and cheap ionic liquid to purify gasolina octane boosters. *Green Chem.* **2007**, *9*, 247–253.
(12) Hunger, J.; Stoppa, A.; Buchener, R. Dipole correlations in the ionic liquid 1-*N*-ethyl-3-*N*-methylimidazolium ethylsulfate and its binary mixtures with dichloromethane. *J. Phys. Chem. B* **2009**, *113*, 9527–9537.
(13) Esser, J.; Wasserscheid, P.; Jess, A. Deep desulphurization on oil refinery streams by extraction with ionic liquids. *Green Chem.* **2004**, *6*, 316–322.
(14) Arce, A.; Earle, M. J.; Rodriguez, H.; Seddon, K. R.; Soto, A. 1-ethyl-3-methylimidazolium bis {(trifluoromethyl)sulfonyl}amide as solvent for the separation of aromatic and aliphatic hydrocarbons by liquid extraction: extensión to C-7 and C-8-fractions. *Green Chem.* **2008**, *10*, 1294–1300.
(15) Meinsdersma, G. W.; Podt, A. J. G.; De Haan, A. B. S. In *Ionic Liquids III: Fundamentals, Progress, Challenges, and Opportunities*; Rogers, R. D., Seddon, K., Eds.; ACS Symposium Series 901−902; American Chemical Society: Washington, DC, 2005; Vol. B, Chapter 5, pp 57−71.
(16) Meinsdersma, G. W.; Podt, A. J. G.; De Haan, A. B. S. Ternary liquid-liquid equilibria for mixtures of toluene + *n*-heptane + an ionic liquid. *Fluid Phase Equilib.* **2006**, *247*, 158–168.
(17) Deenadayalu, N.; Ngcongo, K. C.; Letcher, T. M.; Ramjugernath, D. Liquid-liquid equilibria for ternary mixtures (an ionic liquid + benzene + heptane or hexadecane) at $T = 298.2$ K and atmospheric pressure. *J. Chem. Eng. Data* **2006**, *51*, 988–991.
(18) Gonzalez, E. J.; Calvar, N.; González, B.; Dominguez, A. (Liquid-liquid) equilibria for ternary mixtures of (alkane + benzene + [EMpy][ESO4]) at several temperaturas and atmospheric pressure. *J. Chem. Thermodyn.* **2009**, *41*, 1215–1221.
(19) Gonzalez, E. J.; Calvar, N.; González, B.; Dominguez, A. Liquid-liquid equilibrium for ternary mixtures of hexane + aromatic compounds + [EMpy][ESO4]) at $T = 298.15$ K. *J. Chem. Eng. Data* **2010**, *55*, 633–638.
(20) Gonzalez, E. J.; Calvar, N.; González, B.; Dominguez, A. Separation of toluene from alkanes using 1-ethyl-3-methylpyridinium ethylsulfate ionic liquid at $T = 298.15$ K and atmospheric pressure. *J. Chem. Thermodyn.* **2010**, *42*, 752–757.
(21) Gómez, E.; González, B.; Domínguez, A.; Tojo, E.; Tojo, J. Dynamic viscosities of a series of 1-alkyl-3-methylimidazolium chloride ionic liquids and their binary mixtures with water at several temperatures. *J. Chem. Eng. Data* **2006**, *51*, 696–701.
(22) Gómez, E.; González, B.; Calvar, N.; Tojo, E.; Domínguez, A. Physical properties of pure 1-ethyl-3-methylimidazolium ethylsulfate and its binary mixtures with ethanol and water at several temperatures. *J. Chem. Eng. Data* **2006**, *51*, 2096–2102.
(23) González, B.; Calvar, N.; Gómez, E.; Macedo, E. A.; Domínguez, A. Synthesis and physical properties of 1-ethyl 3-methylpyridinium ethylsulfate and its binary mixtures with ethanol and water at several temperatures. *J. Chem. Eng. Data* **2008**, *53*, 1824–1828.
(24) González, B.; Calvar, N.; Gómez, E.; Domínguez, A. Physical properties of the ternary system (ethanol+water+1-butyl-3-methylimidazolium methylsulphate) and its binary mixtures at several temperatures. *J. Chem. Thermodyn.* **2008**, *40*, 1274–1281.
(25) Gómez, E.; González, B.; Calvar, N.; Domínguez, A. Excess molar properties of ternary system (ethanol+water+1,3-dimethylimidazolium methylsulphate) and its binary mixtures at several temperatures. *J. Chem. Thermodyn.* **2008**, *40*, 1208–1216.
(26) González, B.; Calvar, N.; Gómez, E.; Dominguez, I.; Domínguez, A. Synthesis and physical properties of 1-ethylpyridinium ethylsulfate and its binary mixtures with ethanol and 1-propanol at several temperatures. *J. Chem. Eng. Data* **2009**, *54*, 1353–1358.
(27) Gómez, E.; Calvar, N.; Domínguez, A.; Macedo, E. A. Synthesis and temperature dependence of physical properties of four new pyridinium-based ionic liquids: Influence of the size of the cation. *J. Chem. Thermodyn.* **2010**, *42*, 1324–1329.
(28) Fredlake, C. P.; Crosthwaite, J. M.; Hert, D. G.; Aki, S. N. V. K.; Brennecke, J. F. Thermophysical properties of imidazolium-based ionic liquids. *J. Chem. Eng. Data* **2004**, *49*, 954–964.
(29) Crosthwaite, J. M.; Muldoon, M. J.; Dixon, J. K.; Anderson, J. L.; Brennecke, J. F. Phase transition and decomposition temperatures, heat capacities and viscosities of pyridinium ionic liquids. *J. Chem. Thermodyn.* **2005**, *37*, 559–568.
(30) Seddon, K. R.; Starck, A. S.; Torres, M. J. *Viscosity and density of 1-alkyl-3-methylimidazolium ionic liquids III: Fundamentals, progress, challenges and opportunities.*; ACS Symposium Series 901; American Chemical Society: Washington DC, 2004.
(31) Wilkes, J. S. Properties of ionic liquid solvents for catalysis. *J. Mol. Catal. A: Chem.* **2004**, *214*, 11–17.
(32) Okoturo, O. O.; Vandernoot, J. J. Temperature dependence of viscosity for room temperature ionic liquids. *J. Electroanal. Chem.* **2004**, *568*, 167–181.
(33) Tariq, M.; Forte, P. A. S.; Costa, M. F.; Canongia, J. N.; Rebelo, L. P. N. Densities and refractive indices of imidazolium- and phosphonium-based ionic liquids: Effect of temperature, alkyl chain length, and anion. *J. Chem. Thermodyn.* **2009**, *41*, 790–798.

Received for review June 8, 2010. Accepted November 23, 2010. The authors are grateful to the Ministerio de Educación y Ciencia of Spain (projects CTQ2007-61272, CTQ2007-61788, Ramón y Cajal Program RYC-2008-02388), to the CEE (MINILUBES proyect, PITN-GA-2008-216011), to the Pos-doc scholarships from Fundação para a Ciência e a Tecnologia (FCT, Portugal) (ref SFRH/BDP/48210/2008), to the Xunta de Galicia (project PGIDIT04BTF301031PR), and to the LSRE financing by FEDER/POCI/2010, for financial support.

JE1006357